Development 127, 3855-3864 (2000)
Printed in Great Britain © The Company of Biologists Limited 2000
DEV8749

A phospholipid kinase regulates actin organization and intercellular bridge formation during germline cytokinesis

Julie A. Brill[1,2,§,¶], Gary R. Hime[1,*], Manuela Scharer-Schuksz[1,‡] and Margaret T. Fuller[1]

[1]Departments of Developmental Biology and Genetics, Stanford University School of Medicine, Stanford, CA 94305, USA
[2]Department of Zoology, University of Washington, Seattle, WA 98195, USA
*Present address: University of Melbourne. Parkville VIC 3052, Australia
‡Present address: The Scripps Research Institute, 10550 N. Torrey Pines Rd, La Jolla, CA 92037, USA
§Address as of January 2001: Research Institute, The Hospital for Sick Children, 555 University Avenue, Toronto, Ontario M5G 1X8, Canada.
¶Author for correspondence (e-mail: brill@u.washington.edu)

Accepted 7 June; published on WWW 9 August 2000

SUMMARY

The endgame of cytokinesis can follow one of two pathways depending on developmental context: resolution into separate cells or formation of a stable intercellular bridge. Here we show that the *four wheel drive* (*fwd*) gene of *Drosophila melanogaster* is required for intercellular bridge formation during cytokinesis in male meiosis. In *fwd* mutant males, contractile rings form and constrict in dividing spermatocytes, but cleavage furrows are unstable and daughter cells fuse together, producing multinucleate spermatids. *fwd* is shown to encode a phosphatidylinositol 4-kinase (PI 4-kinase), a member of a family of proteins that perform the first step in the synthesis of the key regulatory membrane phospholipid PIP2. Wild-type activity of the *fwd* PI 4-kinase is required for tyrosine phosphorylation in the cleavage furrow and for normal organization of actin filaments in the constricting contractile ring. Our results suggest a critical role for PI 4-kinases and phosphatidylinositol derivatives during the final stages of cytokinesis.

Key words: Phosphatidylinositol 4-kinase, Actin, Cytokinesis, PIP2, *Drosophila*

INTRODUCTION

In metazoan organisms, cytokinesis is initially driven by the purse-string-like constriction of an actomyosin-based contractile ring and its associated plasma membrane. At the end of cytokinesis, the contractile ring disassembles and the two daughter cells separate (reviewed in Satterwhite and Pollard, 1992; Fishkind and Wang, 1995). Although a large number of protein effectors of cytokinesis have been characterized, crucial mechanistic aspects of the process remain unexplained. For example, it is not clear how filamentous actin (F-actin), myosin II and other cleavage furrow proteins are assembled at the equator of the cell (for review, see Field et al., 1999), how the contractile ring maintains its association with the cell cortex during furrowing, nor how the terminal stage of cytokinesis, which requires proteins distinct from those involved in the previous steps, is regulated (Adachi et al., 1997; Madaule et al., 1998; Powers et al., 1998; Raich et al., 1998; Swan et al., 1998).

A remarkable variation of the universal process of cytokinesis occurs during gametogenesis in many organisms: instead of separating, the daughter cells develop as a syncytium, with clonally related cells connected by intercellular bridges called ring canals (Cooley, 1995). During cytoplasmic bridge formation in the *Drosophila* male germline, structural proteins normally associated with the contractile ring persist to line the ring canal wall. These include the actin-binding protein anillin, and the septins, homologs of yeast bud neck filament proteins (Field and Alberts, 1995; Longtine et al., 1996; Hime et al., 1996). Although F-actin and myosin II are present in constricting contractile rings, they are largely disassembled during intercellular bridge formation in the male germline and do not persist as major components of the resulting ring canals (Hime et al., 1996).

Incomplete cytokinesis in the male germline of *Drosophila* occurs following each of the four mitotic and two meiotic divisions, resulting in syncytial cysts of 64 spermatids connected by 63 ring canals (Lindsley and Tokuyasu, 1980). During meiosis, each primary spermatocyte undergoes two meiotic divisions to generate four early round spermatids, each with a single haploid nucleus. Immediately after meiosis, all of the mitochondria in a spermatid cell aggregate and fuse to form a single mitochondrial derivative (reviewed in Lindsley and Tokuyasu, 1980; Fuller, 1993). Early round spermatids from males defective in meiotic cytokinesis, for example *klp3A* or *tsr*, or treated with the anti-microfilament agent cytochalasin B exhibit a ‘four wheel drive’ phenotype, in which four haploid nuclei accompany an abnormally large mitochondrial derivative (Gunsalus et al., 1995; Williams et al., 1995; Giansanti et al., 1998).

Here we describe *four wheel drive* (*fwd*), a gene required

for proper organization of the constricted F-actin ring, accumulation of phosphotyrosine epitopes, and formation of stable intercellular bridges during male meiosis in *Drosophila*. The *fwd* gene encodes a predicted phosphatidylinositol 4-kinase (PI4K), the enzyme that performs the first committed step in the synthesis of the important membrane phospholipid phosphatidylinositol 4,5-bisphosphate (PIP2). Our results suggest a crucial role for phosphoinositide synthesis in regulating membrane and cytoskeletal dynamics during the endgame of cytokinesis.

MATERIALS AND METHODS

Fly strains and husbandry

Flies were raised on standard cornmeal molasses agar at 25°C (Ashburner, 1990). Visible markers, balancer chromosomes and large chromosomal deletions are described in Lindsley and Zimm (1992). *Df(3L)B71* is the deficiency segregant of *T(Y;3)B71*. The fwd^1 allele was identified as a male sterile mutation in an insertional mutagenesis screen (Cooley et al., 1988). However, detailed deletion mapping revealed that the P element in the line was not associated with the lesion in fwd^1. Four additional EMS-induced alleles ($fwd^{2\text{-}5}$) were isolated from 2377 mutagenized third chromosomes tested for failure to complement fwd^1 in the screen described by Lin et al. (1996). *fwd* alleles were maintained over *TM6B* or *TM6C*.

Small deficiencies in the region were generated by transposase-induced mobilization of two different P elements by the method of Zhang and Spradling (1993). *l(3)10512*, a *PZ* element located in *trachealess* (Isaac and Andrew, 1996), was used to generate *Df(3L)7C*. *0751/02*, a non-lethal *PlacW* insertion in 61B (Deak et al., 1997), was used to generate *Df(3L)17E* and *Df(3L)2D*. The source of transposase for these screens was a TM3 balancer chromosome carrying Δ2-3 on a defective Hobo element (gift of W. Gelbart).

fwd mutant phenotypes were evaluated in males bearing allele/*Df* combinations. Data for $fwd^2/Df(3L)emc^{E12}$ are shown in Figs 1-4. Detailed examination of $fwd^3/Df(3L)emc^{E12}$ and $fwd^5/Df(3L)emc^{E12}$ was also carried out and revealed no appreciable differences. In the experiments in Table 1 and Fig. 7B-E, *Df(3L)7C* was used in place of $Df(3L)emc^{E12}$. The subtle phenotypic differences between fwd^2 and fwd^3 versus fwd^4 and fwd^5 in Table 1 were most likely due to a difference in background chromosomes (see Molecular Biology, below). *Oregon R* was used as the wild-type control for the phenotypic analysis. Viability counts in Table 1 were obtained by counting male progeny from crosses of *fwd* allele/*TM6C* or *Df(3L)17E*/*TM6C* with *Df(3L)7C*/*TM6C* flies. At least 690 flies were counted for each cross. Germline-deficient flies used for northern analysis (Fig. 7A) were obtained as progeny of *oskar* mutant mothers (Lehmann and Nusslein-Volhard, 1986).

Microscopy

Squashed testis preparations were performed as described in Regan and Fuller (1990). The data in Table 1 were obtained by counting early spermatids in ten testes. Fidelity of karyokinesis was assessed by examining the relative sizes of nuclei in early round spermatids (Gonzalez et al., 1989). To view live spermatocytes undergoing cytokinesis, flies were dissected on a coverslip under Voltalef 20S halocarbon oil and spermatocytes were visualized using phase-contrast microscopy essentially as described in Church and Lin (1985) except with an upright microscope (Zeiss Axiophot). Meiotic cells from three (wild type) or four (*fwd*) males were examined, and images were recorded at five-minute intervals using Kodak T-Max 100 film. For immunofluorescence staining, testis sample preparation and rhodamine phalloidin and antibody sources and dilutions were exactly as described (Hime et al., 1996). Images were captured using a Photometrics cooled CCD camera connected to a Zeiss Axiophot microscope (kindly made available by Bruce Baker). Images of separate fluorochromes from multiply-stained tissues were collected individually and combined using Adobe Photoshop.

Molecular biology

Genomic DNA sequences flanking the breakpoints of *Df(3L)7C*, *Df(3L)17E* and *Df(3L)2D* were cloned by plasmid rescue of the P elements used to generate the deficiencies (Uemura et al., 1989; Preston et al., 1996). Fourteen genomic phage forming a contiguous walk across the *Df(3L)7C* interval (spanning approximately 80 kilobases (kb)) were isolated from the Tamkun λEMBL3 library (Tamkun et al., 1992) by hybridization with the following probes: 0.8 kb flanking the *Df(3L)7C* distal breakpoint; the 3.5 kb *Eco*RI fragment from cosmid 13C12 (European Drosophila Genome Project; EDGP); the 4.7 kb *Xba*I fragment from cosmid 146B11 (EDGP); and a 2.3 kb *Not*I-*Nco*I end fragment from an *Nco*I deletion derivative of P1 DS00539 (Berkeley Drosophila Genome Project; BDGP). Southern blots and other molecular techniques were carried out essentially as described in Sambrook et al. (1989). Radioactive probes were labeled with [α-^{32}P]dCTP (NEN) using the Megaprime or Rediprime kits (Amersham). Poly (A)+ RNA for northern blots (Fig. 7A) was purified from whole RNA made using the Trizol Reagent (Gibco/BRL) by batch binding to oligo(dT) cellulose (Pharmacia). *Bam*HI fragments used as probes on Southern and northern blots are indicated (*,**, Fig. 5B). The ribosomal protein probe Rp49 was from a plasmid kindly provided by M. Schubiger and S. McNabb (O'Connell and Rosbash, 1984).

Sequencing reactions were carried out using the Big Dye kit (Amersham) on a Perkin Elmer 9600 GeneAmp PCR machine, using primers obtained from Operon (Emeryville, CA). Unincorporated nucleotides were removed using Autoseq G-50 columns (Pharmacia) and reactions were run on an ABI sequencer at the Biochemistry Sequencing facility (University of Washington). Sequencing of *fwd* alleles was carried out on aggregate PCR products pooled from at least two independent reactions. Genomic DNA isolated from *fwd*/*Df* males was amplified using the *Pfu* Turbo enzyme (Stratagene) and pairs of sequencing primers. For each allele, 7-10 overlapping PCR products spanning 6.1 kb of contiguous genomic DNA were sequenced, including all but approx. 100 nucleotides at the C terminus of the predicted protein. The genomic sequences of fwd^2 and fwd^3 differed from fwd^4 and fwd^5 in a manner consistent with different respective background chromosomes (data not shown). PCR products and probe fragments were gel purified using the Qiaquick kit (Qiagen). Homology searches and sequence comparisons used the BLAST and ClustalW programs on the NCBI and BCM web sites, respectively. Accession numbers of the proteins compared in Fig. 8 were *fwd* (AF242375), *H. sapiens* (AAC51156), *A. thaliana* (CAB37928), *C. elegans* (AAA83177), *D. discoideum* (AAA85725), *S. pombe* (CAA93903) and *S. cerevisiae* (CAA96174).

cDNAs corresponding to ESTs in the Berkeley Drosophila Genome Project database that matched the genomic sequence were purchased from Research Genetics (GH11214, GM01278, GM08014, LD25627) and Genome Systems, Inc. (LD5780, LD06959, LD07966, LD29916). The 5′ ends of these cDNAs show evidence for alternative splicing, resulting in alternate amino-terminal predicted amino acid sequences in a non-conserved part of the protein (data not shown). The predicted protein sequence shown in Fig. 6 is from GH11214, a cDNA from the head EST library (BDGP) that contains in-frame stop codons in the 5′ untranslated region upstream of the first methionine. Partial cDNAs were also obtained by screening the BS testis cDNA library (generously provided by J. Andrew and B. Oliver) with the 1.3 kb *Bam*HI genomic fragment (*, Fig. 5B) and with an 0.8 kb *Sal*I fragment internal to the 3.0 kb *Bam*HI fragment (**, Fig. 5B). The most amino-terminal amino acid from a conceptual translation of the partial testis cDNAs is aa191 of the sequence shown in Fig. 6. The rest of the testis cDNA sequence produced a predicted protein nearly identical to that shown in Fig. 6, except for several conservative amino

acid substitutions, reflecting the different strain backgrounds used to make the two libraries (data not shown).

RNA in situ hybridization was carried out as described (White-Cooper et al., 1998), using as probes DIG-labeled (Boehringer-Mannheim) single-stranded sense and antisense products made with T3 (Boehringer-Mannheim) or T7 (New England Biolabs) polymerases, respectively, from LD06959. This cDNA includes 4.0 kb that is common to all of the cDNA clones (see above) and would be expected to hybridize to all known alternative transcripts. Testes were photographed on a Nikon Microphot-FX microscope with DIC optics (kindly made available by Gerold Schubiger).

RESULTS

four wheel drive (*fwd*) is required for late stages of cytokinesis during male meiosis

Males mutant for *fwd* had abnormal early round spermatids, suggesting a defect in cytokinesis during male meiosis. In wild-type early round spermatids, the haploid nucleus and the mitochondrial derivative in each cell appeared approximately the same diameter in unfixed squashed preparations viewed by phase-contrast microscopy (Fig. 1A). In testes from flies bearing either EMS-induced mutant alleles of *fwd* or a deletion of the entire gene, early round spermatids commonly contained four (or, less often, two) normal-sized nuclei associated with an abnormally large mitochondrial derivative (Fig. 1; Table 1). The spermatids with four nuclei and a large mitochondrial derivative (Fig. 1B) most likely resulted from failure of cytokinesis at both meiotic divisions followed by the aggregation and fusion of mitochondrial material equivalent to that of four cells. Spermatids with two nuclei and an intermediate-sized mitochondrial derivative (Fig. 1B) most likely failed cytokinesis at only one of the two meiotic divisions. Spermatids with one nucleus and a mitochondrial derivative of similar size, suggesting successful meiosis, were rare in the mutants. The nuclei observed in all cells were normal in size, indicating that karyokinesis was unaffected by mutations in *fwd*.

Occasionally cells were observed with nucleus:mitochondrial derivative ratios other than 1:1, 2:1 or 4:1 (Table 1). Cells with three nuclei per mitochondrial derivative could have arisen from successful separation of a single spermatid during meiosis II from a cell that had failed cytokinesis during meiosis I. Cells containing 8 or 16 (or, more rarely, 6 or 12) haploid nuclei associated with extremely enlarged mitochondrial derivatives probably derived from failure of one or more of the preceding mitotic divisions in addition to failure of meiosis I and meiosis II (Table 1, c.f. fwd^{4}/*Df(3L)7C*, fwd^{5}/*Df(3L)7C*, *Df(3L)17E*/*Df(3L)7C*). Indeed, primary spermatocytes with two sets of prometaphase chromosomes were occasionally observed in orcein-stained squashed preparations (data not shown).

The phenotype of failure of meiotic cytokinesis in *fwd* mutants was highly penetrant; greater than 99% of haploid nuclei observed were in multinucleate spermatids (Table 1). All five alleles of *fwd*, one from a P-element screen (fwd^{1}) and four obtained by EMS mutagenesis (fwd^{2-5}), showed similar phenotypes as hemizygotes (allele/Df; Table 1). The mutants appeared to be null alleles, as a viable combination of deletions (*Df(3L)17E*/*Df(3L)7C*) that removed the entire *fwd* gene had a similar cytokinesis defect (Table 1).

The spermatogenesis defect in the *fwd* mutants appeared to be restricted to cytokinesis, in that there was no arrest of spermiogenesis in *fwd* males. Indeed, flagellar elongation (Fig. 1D) and nuclear shaping (not shown) appeared morphologically normal. All late-stage spermatid bundles were extensively elongated, although the spermatids within the bundles appeared thick and irregularly packed (compare Fig. 1E,F). Cross-sections of elongating spermatids examined by transmission electron microscopy revealed sets of two or four axonemes accompanying enlarged mitochondrial derivatives, consistent with the formation of multinucleate cells (data not shown). No motile sperm were observed, as *fwd* spermatids failed individualization. In addition, although all *fwd* mutant males examined exhibited severe meiotic cytokinesis defects and were sterile, females mutant for *fwd* were fertile and showed no obvious defects in oogenesis when ovarioles were examined by light microscopy (data not shown). *fwd* flies of both sexes were fully viable (males, Table 1; females, not shown).

To determine the stage of meiotic cytokinesis affected in *fwd* mutants, we viewed living cells from wild-type and *fwd* mutant

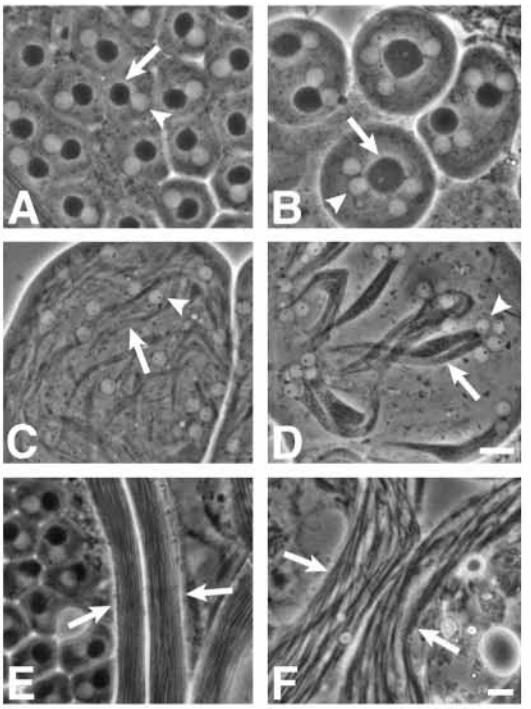

Fig. 1. *fwd* spermatids commonly have four nuclei associated with a large mitochondrial derivative. Phase-contrast light micrographs of post-meiotic spermatids in unfixed squashed preparations of (A,C,E) wild-type (*Oregon R*) and (B, D,F) *fwd* mutant (fwd^{2}/*Df(3L)emc*^{E12}) testes. Arrowheads, nuclei; Arrows, mitochondrial derivatives. (A,B) Onion-stage spermatids. Note presence of two or four nuclei per mitochondrial derivative in *fwd*. (C,D) Early elongating spermatids. A pair of elongating mitochondrial derivatives (arrow) is associated with each nucleus (C, arrowhead) or each set of nuclei (D, arrowhead). Note the enlarged mitochondrial derivatives (arrow) associated with four nuclei (arrowhead) in *fwd* (B,D). (E,F) Elongating spermatid bundles. Each arrow points to a bundle of spermatids. Note the parallel arrays of sperm tails in wild type (E) as compared to the disorganized bundles in *fwd* (F). Scale bars, A-D and E,F, 10 μm.

Table 1. *fwd* alleles show a high frequency of cytokinesis failure during male meiosis

Genotype	Number of cells with the indicated ratio of haploid spermatid nuclei per mitochondrial derivative*								Total nuclei	Percentage defective§	Percentage viability¶
	1:1	2:1	3:1	4:1	6:1	8:1	12:1	16:1			
Df(3L)7C / TM6C	1501	2	0	0	0	0	0	0	1505	0.3	100.0
fwd^{1} / *Df(3L)7C*	3	14	0	302	0	15	0	0	1359	99.8	98.2
fwd^{2} / *Df(3L)7C*	14	112	8	272	0	2	0	0	1366	99.0	103.1
fwd^{3} / *Df(3L)7C*	11	97	7	310	0	3	0	0	1490	99.3	113.8
fwd^{4} / *Df(3L)7C*	3	40	2	254	1	19	1	1	1291	99.8	96.4
fwd^{5} / *Df(3L)7C*	3	41	1	297	2	7	2	2	1400	99.8	86.2
Df(3L)17E / Df(3L)7C	12	88	7	285	2	12	1	1	1485	99.2	66.1

*Measured by counting cells in live squashed preparations (see Materials and Methods). Because cell membranes are often disrupted by squashing (Cenci et al., 1994; Hime et al., 1996), the number of cells reported is actually the number of mitochondrial derivatives examined.

§Expressed as the percentage of spermatid nuclei derived from one or more defective meiotic and/or mitotic divisions.

¶Expressed as a percentage of the expected number of test class progeny (see Materials and Methods).

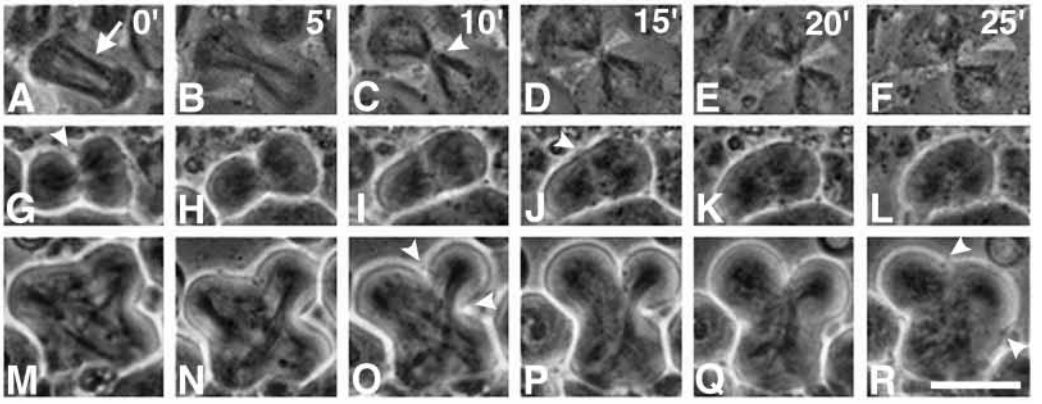

Fig. 2. *fwd* cells fail to establish stable intercellular bridges after meiotic division. Time-lapse photographs of living (A-F) wild-type (*Oregon R*) and (G-R) *fwd* mutant (*fwd*^{2}*/Df(3L)emc*^{E12}) secondary spermatocytes undergoing meiosis II. Panels in each set are consecutive images taken at 5 minute intervals. Cells undergoing meiotic division can be identified by the presence of phase-dark mitochondria that align along the spindle (arrow, A). (A-F) Wild-type cell. Note the appearance (arrowhead, C) of a cleavage furrow separating the daughter cells. The furrow was maintained for at least 15 minutes (F). (G-R) *fwd* mutant (*fwd*^{2}*/Df(3L)emc*^{E12}) cells. (G-L) Cell that had successfully completed meiosis I and was undergoing meiosis II. (M-R) Cell that had failed to separate the daughter cells during meiosis I and was undergoing meiosis II with two spindles contained within a single cytoplasm. In *fwd* cells, cleavage furrows formed (arrowheads, G,O) but were not maintained, and daughter cells fused together within fifteen minutes (arrowheads, J,R). Scale bar, 10 μm.

testes dissected under oil (see Materials and Methods). Cells undergoing meiotic division are easily identified by the phase-dark mitochondria, which line up along the meiotic spindle (Fig. 2A, arrow). In nearly all (12/13) wild-type cells undergoing cytokinesis during either meiosis I or meiosis II, cleavage furrows ingressed, bisected the cell at the equator (Fig. 2C, arrowhead) and persisted for the remainder of the observation period (at least fifteen minutes; Fig. 2C-F). The remaining cell did not form a cleavage furrow within the time frame of the observation. In the majority of *fwd* mutant cells (13/15; Fig. 2G-R), cleavage furrows initiated and ingressed (Fig. 2G,O, arrowheads), as in wild type. In five of these 13 cells (38%), the cleavage furrows did not persist and the daughter cells fused back together within 15 minutes (Fig. 2I,R), suggesting a role for *fwd* in stable intercellular bridge formation. The remaining eight *fwd* cells formed stable cleavage furrows. However, five of these cells had failed a previous division, as assessed by the presence of two or more nuclei in each of the daughter cells (not shown). Of the two *fwd* cells that did not form a detectable cleavage furrow, one had failed multiple previous divisions, as it contained six nuclei (not shown). These data likely underestimate the frequency of cytokinesis failure in *fwd*, as grossly abnormal structures deriving from defects in multiple earlier divisions were not scored in the analysis. Consistent with formation and ingression of cleavage furrows observed in living *fwd* cells, fluorescence microscopy revealed that early stages of cytokinesis appeared normal in *fwd* mutant cells. F-actin, myosin II, anillin and pnut, one of the septins, showed wild-type distribution in the cleavage furrow during late anaphase and early telophase (Hime et al., 1996; data not shown).

Tyrosine phosphorylation and normal F-actin organization in the cleavage furrow require *fwd*

In wild type, phosphotyrosine (P-tyr) epitopes accumulate at the site of the arrested cleavage furrow late in cytokinesis in dividing male germ cells and persist to mark the ring canal walls after both the mitotic and meiotic divisions (Hime et al., 1996). P-tyr epitopes initially appear during late anaphase and early telophase as punctate spots in the partially constricted cleavage furrow. These spots gradually coalesce to form a tight band coincident with F-actin in the constricted contractile ring (Fig. 3A, arrow; Hime et al., 1996). Of 63 wild-type telophase cells examined, 57 (91%) showed P-tyr epitopes associated with the F-actin contractile ring. The remaining six cells, although in telophase, may have been at too early a stage of constriction for accumulation of P-tyr epitopes. In 48/63 (76%)

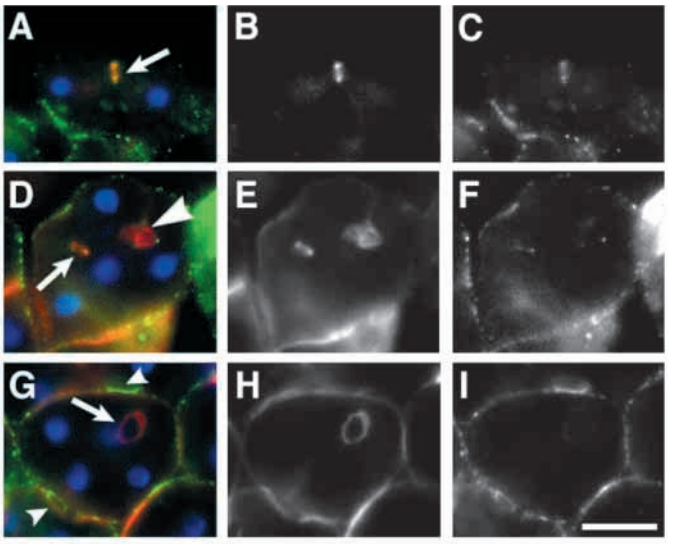

Fig. 3. Wild-type *fwd* function is required for appearance of phosphotyrosine epitopes late in cytokinesis. (A-I) Phosphotyrosine (green) accumulation compared to actin (red) in the constricted contractile ring. (A,D,G) Superimposed CCD images (blue DNA), with (B,E,H) actin and (C,F,I) phosphotyrosine staining shown separately. Arrows and large arrowhead, constricting contractile rings. (A-C) Wild-type late telophase II. Phosphotyrosine epitopes form a ring coincident with the constricted contractile ring (arrow). (D-F) Mutant ($fwd^2/Df(3L)emc^{E12}$) late telophase II showing a ring of phosphotyrosine (arrow) or only a few spots of anti-phosphotyrosine staining (arrowhead) in the vicinity of the constricted contractile rings. Note the delocalization of actin in one of the contractile rings (arrowhead). The two contractile rings shown here represent the entire range of the P-tyr phenotype described in the text. (G-I) Mutant ($fwd^2/Df(3L)emc^{E12}$) meiosis II cell undergoing cytokinesis with at most three dots of phosphotyrosine staining (I) detected in the vicinity of the constricting contractile ring (H). Ring canal walls from preceding mitotic divisions contained phosphotyrosine epitopes but no F-actin (arrowheads, G). Note that the squash technique used for sample preparation does not preserve plasma membrane association with the contractile ring, even in wild type (Cenci et al., 1994; Hime et al., 1996). Scale bar, 10 μm.

of wild-type cells, P-tyr epitopes were present in a smooth ring that colocalized with the F-actin contractile ring. In *fwd* mutant telophase cells, by contrast, only 35/64 (55%) of the contractile rings had associated P-tyr epitopes and, for most of these (29/64 cells; 45%), the P-tyr staining was usually only a few dots (Fig. 3D, arrowhead; Fig. 3G, arrow). A smooth ring of P-tyr epitopes was observed in only six *fwd* cells (9%; c.f. Fig. 3D, arrow). Rings of P-tyr failed to accumulate even in *fwd* mutant dividing spermatocytes with tightly constricted contractile rings (Fig. 3D, arrowhead). In contrast, intercellular bridges that had formed successfully during the preceding mitotic divisions in the mutants contained smooth rings of P-tyr epitopes that, like mature ring canals in wild type, lacked F-actin (Fig. 3G, arrowheads).

fwd function is required for normal F-actin distribution in the constricted contractile ring. In wild-type cells undergoing meiosis, F-actin and myosin II remained tightly colocalized in the constricting contractile ring (Fig. 4A, arrow; Hime et al., 1996) However, in *fwd*, aberrant accumulations of F-actin appeared in the vicinity of the constricted contractile ring in late telophase (Fig. 4D, arrow; see also 3D, arrowhead). In these abnormal contractile rings, only a small fraction of the total F-actin colocalized with myosin II (Fig. 4D). The frequency of the defect in F-actin distribution was evaluated by examining the contractile rings of wild-type and *fwd* late anaphase and telophase cells stained for both F-actin and P-tyr (as in Fig. 3). In only two cases (3%) did the F-actin in the contractile ring appear delocalized in wild type. In contrast, 20/64 (31%) *fwd* cells exhibited aberrant actin accumulations similar to those shown in Figs 3D, 4D. Thus *fwd* mutant cells exhibited a dramatic increase in the frequency of disrupted F-actin organization in constricted contractile rings relative to wild type.

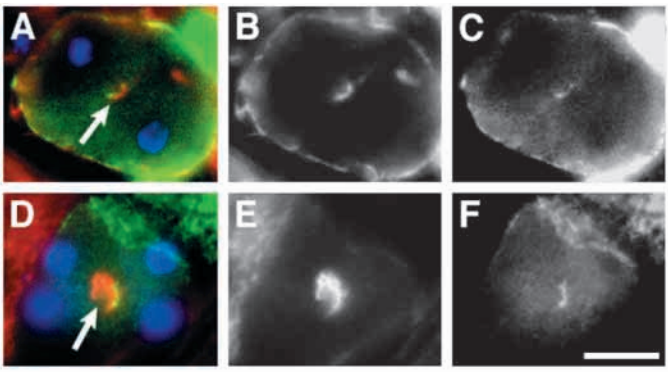

Fig. 4. Wild-type *fwd* function is required for proper actin contractile ring morphology late in cytokinesis. (A-F) Telophase II cells stained for F-actin (red), cytoplasmic myosin II (green) and DNA (blue). (A,D) Superimposed CCD images, with (B,E) F-actin and (C,F) myosin II staining shown separately. (A-C) Wild-type (Oregon R) telophase II. Actin and myosin colocalize in the constricted contractile ring (arrow). Note that half of the contractile ring is out of the plane of focus. (D-F) Late telophase *fwd* mutant cell ($fwd^2/Df(3L)emc^{E12}$) with disorganized F-actin in constricted contractile ring (compare E with B). Scale bar, 10 μm.

fwd encodes a homolog of phosphatidylinositol 4-kinase β (PI4Kβ)

The *fwd* gene was initially localized to polytene interval 61A-C1 by recombination and deficiency mapping (Fig. 5A; recombination data not shown). An interval of approximately 27 kilobases (kb) containing sequences required for *fwd* function was defined by molecular mapping of the distal (telomeric) breakpoint of *Df(3L)7C* and the proximal (centromeric) breakpoint of *Df(3L)17E*, and a series of overlapping genomic phage representing the deficiency interval was isolated and mapped (Fig. 5). Southern blot analysis of wild-type and mutant genomic DNA using a subset of fragments across the 27 kb interval as probes revealed several restriction fragment length polymorphisms (RFLPs) within a 1.2 kb *Sal*I-*Bam*HI fragment (Fig. 5B, gray bar) consistent with a complex rearrangement in the fwd^1 allele (data not shown).

Sequence analysis of a total of 9.6 kb of cloned wild-type genomic DNA around the region of the fwd^1 RFLPs (thick bar, Fig. 5B) revealed a 2.6 kb contiguous open reading frame (ORF) with a significant degree of homology (e^{-50}) to human phosphatidylinositol 4-kinase β (PI4Kβ), including part of the catalytic domain. A predicted protein sequence for *fwd*

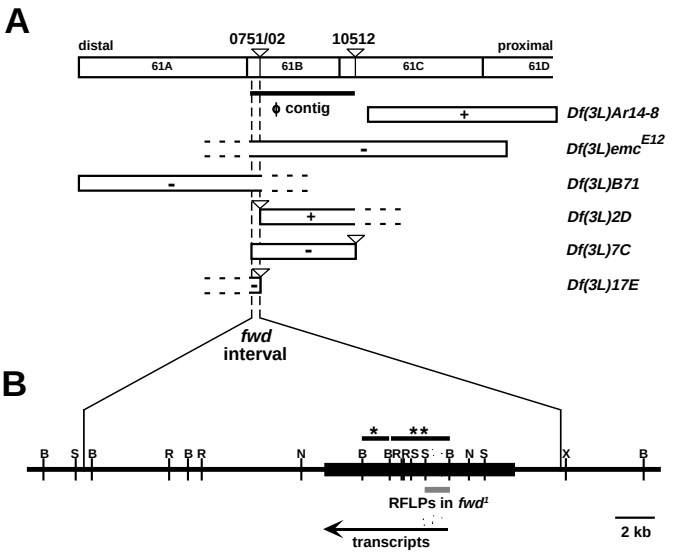

Fig. 5. Cloning of *fwd*. (A) Deficiency map of the *fwd* region. Top line: Polytene chromosome interval 61A-D. Triangles, insertion sites for P elements 0751/02 and *l(3)10512*, which were used to generate small deletions. Bar below polytene map, region spanned by cloned phage contig of genomic DNA. Open boxes, DNA deleted in deficiency stocks (breakpoints not defined molecularly shown as dashes). P elements were retained at breakpoints of small deletions (indicated by triangles). +, complemented *fwd*; –, failed to complement *fwd*; vertical dashed lines, *fwd* interval determined by distal breakpoint of *Df(3L)7C* and proximal breakpoint of *Df(3L)17E*. (B) Genomic DNA containing the *fwd* gene. Restriction map of genomic DNA across *fwd* interval. Distal breakpoint of *Df(3L)7C* and proximal breakpoint of *Df(3L)17E* (from A) are indicated. Restriction enzymes: B, *Bam*HI; R, *Eco*RI; S, *Sal*I; H, *Hin*dIII; X, *Xho*I; N, *Not*I. Thick black box, 9.6 kb of sequenced wild-type genomic DNA; *, 1.3 kb and **, 3.0 kb *Bam*HI fragments used as probes on Southern and northern blots (see Materials and Methods and Fig. 7A). Gray bar, region containing RFLPs indicating rearrangements in the *fwd*^{1} allele; arrow, location of *fwd* transcripts (shown with 5′ end to the right, corresponding to the chromosomal orientation of the transcription unit).

```
   1 MGILLPPVSQ VTNNHINHTQ HHRNRSLDSA LQRIPEVEVS SPNAESENTF CSPSILGATM CSKIATTAAT VTSALSPPGT  80
  81 PTPALMSTAC TPTIGAVKGN VQHPVPKHEQ SISLAAACRS SAVVESCPTL RMRPKSSESV AANGQEMIGV IVSSTGNGSS 160
 161 SSNNSCSSAG STKKREDLTS LGSDDSGIIC GSESDQISLN RICHSHESLD SGEMDADADA EEECVDLMDT TSIDEEYNIM 240
 241 QPDHLCLYPP QAASTELDCR TLRPSRKQKR QQQQVLERKN LPSQNQIESE DSVDAGVDAR TRYRVMNMSQ AAINVELGTA 320
 321 SNEIDPDVNY RESHQDPIAD APSLSTPSVA STASATPSVT PTPIATPTPT ESTKNDQVLF KNFFGATKNA IFRTAQSIIE 400
 401 NHEKKNAAKQ KEQPDHSGTV SLVGSPNGGS SVPQDLVKSP TDISKKKEFF SLLTSSSSIK AAAAAAANSA ASTPPATPTE 480
 481 ALAANSNSKL QPLSDPSADL KVKERTLNLR LPGDSEGSEG ALTKCSSINS IHKLKLPVPG VVKYFISEKA PVSDVLQKPE 560
 561 KGQSGLLRFF ESPVFNIHFA VHYLFYSKEP GVLSFIGNKI FSFPDQEVDL YIPQLVVMYI QMDELAEVLD PYLTIRCRKS 640
 641 VDFSLKCLWL LEAYNYQVDS LGNSHNSSRK SKLALMKEIF SKREHKQTQN DLKSAGTGGL HVEEPRSVVA LAKKTHHRSQ 720
 721 SDATVLLADF RSPHTLSISH RMYQQPPYTT QTLPTTPAKL CLGDLTSGHA FDNGCTCFET VRGQVNGLLG QRTLCSCGAP 800
 801 KTSPQKEFMK ALMNVGKNLT SWPSKAEKTS ALRMSLNLIN KNLPARVWLP LYSDIPHHVV RITEEKTAVL NSKDKTPYII 880
 881 YVEVVEIPDI YTSPLIPKMM PSLRHTKSEE HLDGSCLNSH QHLSCSRTSS CSSSQQGTSC RRKKGADVDG GCGDAGPHNS 960
 961 CSNVHSLGGL QFQEDDVWSQ EEDEITAQYL NMRKVSERDT ISQISLDSCD SRDQGPPVVF NIGDVRLRHC SNLSCENTKS 1040
1041 FSNDPEDPSA AALKEPWHEK EKLIRESSPY GHLSNWRLLS AIVKCGDDLR QELMATQLLQ MFKIIWQEEQ VDLWVRPYKI 1120
1121 VCLSNDSGLI EPILNTVSLH QIKKNSNKSL KEYFIDEYGS PSGESFRRAQ KNFVQSCAAY CLISYLLQVK DRHNGNILFH 1200
1201 SDGHIIHIDF GFILSISPKN LGFEQSPFKL TPEFVEVMGG TSSEHWREFN KLLLVGMMSA RKHMDRIINF VEIMRSNAHL 1280
1281 PCFKNGCSGT VQNLRKRFHM NLTEQEMERK VEQLVQDSLK SLSTKLYDGY QYYTNGIL                         1338
```

Fig. 6. *fwd* encodes a phosphatidylinositol-4 kinase β. Predicted amino acid (aa) sequence of ORF encoded by cDNA GH11214 (see Materials and Methods). Bold, the positions of stop codons and amino acid substitution in *fwd* mutants: Q310 (stop codon in *fwd*^{3}), Q491 (stop codon in *fwd*^{2}), Q720 (stop codon in *fwd*^{4}), S1138 (Phe in *fwd*^{5}). Outlined region, amino acid sequence encoded by DNA used as probe for northern blot (*, Fig. 5B; see Fig. 7A). Gray boxes, aa sequences corresponding to conserved phosphoinositide kinase (PIK; aa 581-659), β signature motif (BSM; aa 808-886) and catalytic (kinase; aa 1082-1338) domains (see text). These sequence data are available from GenBank under accession number AF242375.

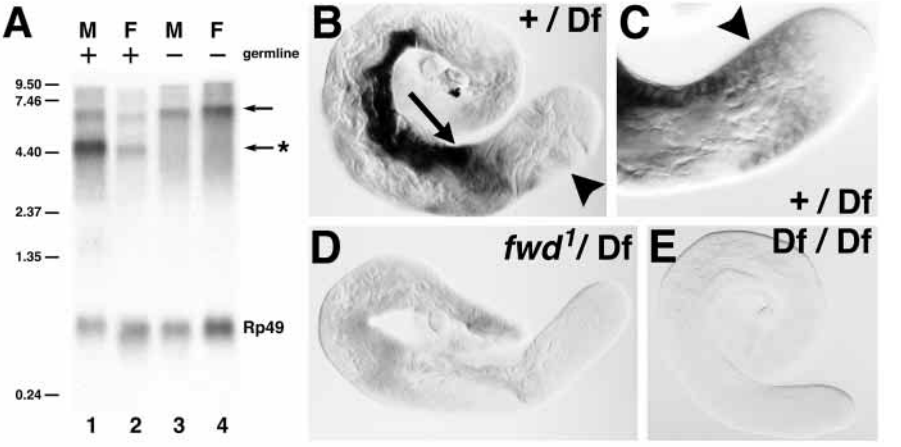

Fig. 7. *fwd* encodes a germline-dependent transcript expressed in primary spermatocytes, meiotic and early post-meiotic male germ cells. (A) Northern blot of poly(A)+ RNA. (Lanes 1-2) Wild-type (Oregon R) (M) males and (F) females. (Lanes 3,4) Germline-deficient (M) males and (F) females. Flies lacking germline were obtained as progeny of *osk* mutant mothers. Probes: *fwd* genomic fragment (1.3 kb *Bam*HI fragment; *, Fig. 5B) and *rp49* as a loading control. Arrows, 6.5-7.0 kb and 4.4 kb (asterisk) transcripts. Molecular weight markers are indicated at left. (B-E) In situ hybridization of an antisense single-stranded RNA probe to whole-mount testes from (B,C) *Df(3L)7C*/TM6C, (D) *fwd*^{1}/*Df(3L)7C* and (E) *Df(3L)17E*/*Df(3L)7C* males (see Materials and Methods). In each panel, the apical tip of the testis (where the germline stem cells are located) is shown on the right. Syncytial cysts of mature primary spermatocytes, meiotic and early postmeiotic cells are found in roughly temporal order moving clockwise along the inner curve of the testis. (B,C) Primary spermatocytes (arrowheads). Note that these are largely out of the plane of focus in B. Higher power magnification view of primary spermatocyte expression in a different testis is shown in C. Arrow, mature primary spermatocytes about to undergo meiosis. Control reactions using the sense strand as probe were indistinguishable from *Df(3L)17E*/*Df(3L)7C* (data not shown).

(Fig. 6) was obtained by conceptual translation of a cDNA identified from an EST that matched the genomic sequence (see Materials and Methods). To confirm that the PI4K gene corresponds to *fwd*, we sequenced 6.1 kb of genomic DNA, including nearly the entire coding region of the gene, from each of the four EMS-induced *fwd* alleles (see Materials and Methods). The fwd^2, fwd^3 and fwd^4 mutations introduced stop codons into the PI4K ORF, whereas the fwd^5 allele carried a Ser→Phe missense mutation at a conserved residue in the PI4K catalytic domain (Fig. 6; mutated residues indicated in bold).

The *fwd* gene may encode both germline-dependent and somatic transcripts. Northern blot analysis of mRNA from whole adult flies using a 1.3 kb *Bam*HI fragment containing 1.2 kb (418 amino acids) of the predicted PI4K ORF as a probe (*, Fig. 5B; outlined region, Fig. 6) revealed a 4.4 kb transcript in males (Fig. 7A). This transcript was present at a lower relative abundance in females (Fig. 7A, compare lanes 1 and 2), and was not detected in males or females lacking a germline (Fig. 7A, lanes 3-4). In addition, a larger germline-independent transcript of approximately 6.5-7.0 kb was detected in both males and females (Fig. 7A). On testis northern blots, the higher molecular weight transcript was not observed. The germline-dependent transcript resolved into a doublet of 4.0 and 4.4 kb that was not detected in testis RNA from fwd^1/Df males, suggesting these transcripts are products of the *fwd* gene (data not shown).

As expected from the requirement for *fwd* function during male meiosis, transcription of *fwd* was detected in primary spermatocytes, late primary spermatocytes, meiotically dividing cells and early round haploid spermatids by in situ hybridization of RNA in whole adult testes (Fig. 7B,C; see Materials and Methods). *fwd* mRNA was detected at lower abundance in the spermatogonial cells at the tip of the testis, but was not detected in bundles of elongating spermatids (data not shown). *fwd* transcripts were nearly undetectable in testes from $fwd^1/Df(3L)7C$ males (Fig. 7D), consistent with results from the northern analysis (see above), and were not detected in testes from flies deleted for the entire *fwd* gene (*Df(3L)17E*/*Df(3L)7C*, Fig. 7E).

Structure of the *fwd* PI4Kβ

Comparison of the predicted protein sequence of the *fwd* PI4Kβ with sequences of PI4Kβs from other species revealed a striking degree of homology in three highly conserved domains in the carboxy (C) terminal half of the predicted protein (Fig. 8A): (1) the PIK (phosphoinositide kinase), also called the LKU (lipid kinase unique), domain, (2) a domain specific to PI4Kβ family members that we have termed the BSM (β signature motif), and (3) the catalytic (kinase) domain. Pairwise comparisons between the *fwd* PI4Kβ and its homologs from other species revealed that the *fwd* protein is most closely related to those from human (Fig. 8A), rat and cow (not shown). The PIK domain is highly conserved (Fig. 8A,B) and is homologous to PIK domains from phosphoinositide 3-kinases and PI4Kαs as well as PI4Kβs (data not shown). The novel BSM, noted previously by Hsuan et al. (1998) and Xue et al. (1999), is also highly conserved (Fig. 8A,C). The BSM lies between the PIK and catalytic domains in all PI4Kβ sequences in the database (Fig. 8A) and appears to be unique to members of the PI4Kβ subfamily of lipid kinases, as it was not found in phosphoinositide 3-kinases or PI4αs (Hsuan et al., 1998; Xue et al., 1999), nor in any other proteins currently in the database. The most striking conservation between the *fwd* protein and PI4Kβs from other species was in the catalytic domain (Fig. 8A,D). The overall structure of many lipid and protein kinases is similar, and the predicted *fwd* kinase domain contains all residues thought, by analogy to protein kinases, to be required for lipid kinase catalytic function (Fig. 8D, asterisks; Gehrmann and Heilmeyer, 1998).

DISCUSSION

fwd PI4K is required for resolution of cytokinesis during male meiosis

Identification of the *fwd* protein as a PI4Kβ homolog indicates an important role for phospholipids in regulating the final stages of cytokinesis. The principal known biochemical function of PI 4-kinases is to convert phosphatidylinositol (PI) to phosphatidylinositol 4-phosphate, or PIP. Subsequent phosphorylation of PIP by PI4 5-kinases results in the formation of the regulatory molecule PIP2. PIP and PIP2 can also be phosphorylated by phosphoinositide 3-kinases to form phosphatidylinositol 3,4-bisphosphate and phosphatidylinositol 3,4,5-trisphoshate (PIP3). PIP2, best known as the precursor of the second messengers inositol trisphosphate and diacylglycerol, has also been shown to interact directly with a number of proteins in the cell, regulating both their localization and activities (see below). Phosphoinositides make up only a small fraction of the membrane lipid molecules in a cell. Local synthesis of phosphoinositides is thought to regulate particular subcellular processes (reviewed in Godi et al., 1999). Due to their subcellular compartmentalization (see below), PI4Ks can be thought of as localized gatekeepers for PIP and PIP2 accumulation.

Although *PIK1*, the budding yeast homolog of *fwd*, is an essential gene (Flanagan et al., 1993; Garcia-Bustos et al., 1994), *fwd* is not. Flies carrying overlapping deletions that remove the entire coding region of *fwd* are viable and female fertile. This is particularly surprising given that *fwd* encodes the sole predicted PI4Kβ in the *Drosophila* genome. The *fwd* protein may be redundant with other PI4Ks. Indeed, most eukaryotes possess multiple PI4Ks (reviewed by Balla, 1998; Fruman et al., 1998; Hsuan et al., 1998), including type II (identified only by biochemical activity) as well as type III (now identified by the two cloned isoforms, PI4Kα and PI4Kβ). The domain structure of the mammalian PI4Kα and PI4Kβ proteins is different (in PI4Kα, the PIK domain and the catalytic domain are separated by a pleckstrin homology (PH) domain rather than the BSM; reviewed by Hsuan et al., 1998), yet both classes of proteins carry out similar biochemical activities (reviewed in Fruman et al., 1998). PI4Kα and PI4Kβ have overlapping but distinct subcellular localization patterns in human tissue culture cells (Wong et al., 1997), suggesting that the two isoforms might be redundant for some activities. In *Drosophila*, wild-type function of the *fwd* PI4Kβ could be required for incomplete cytokinesis in the male germline either because the single predicted PI4Kα is not expressed in spermatocytes or because regulatory properties or subcellular distributions distinguish the *fwd* protein from the still uncharacterized PI4Kα.

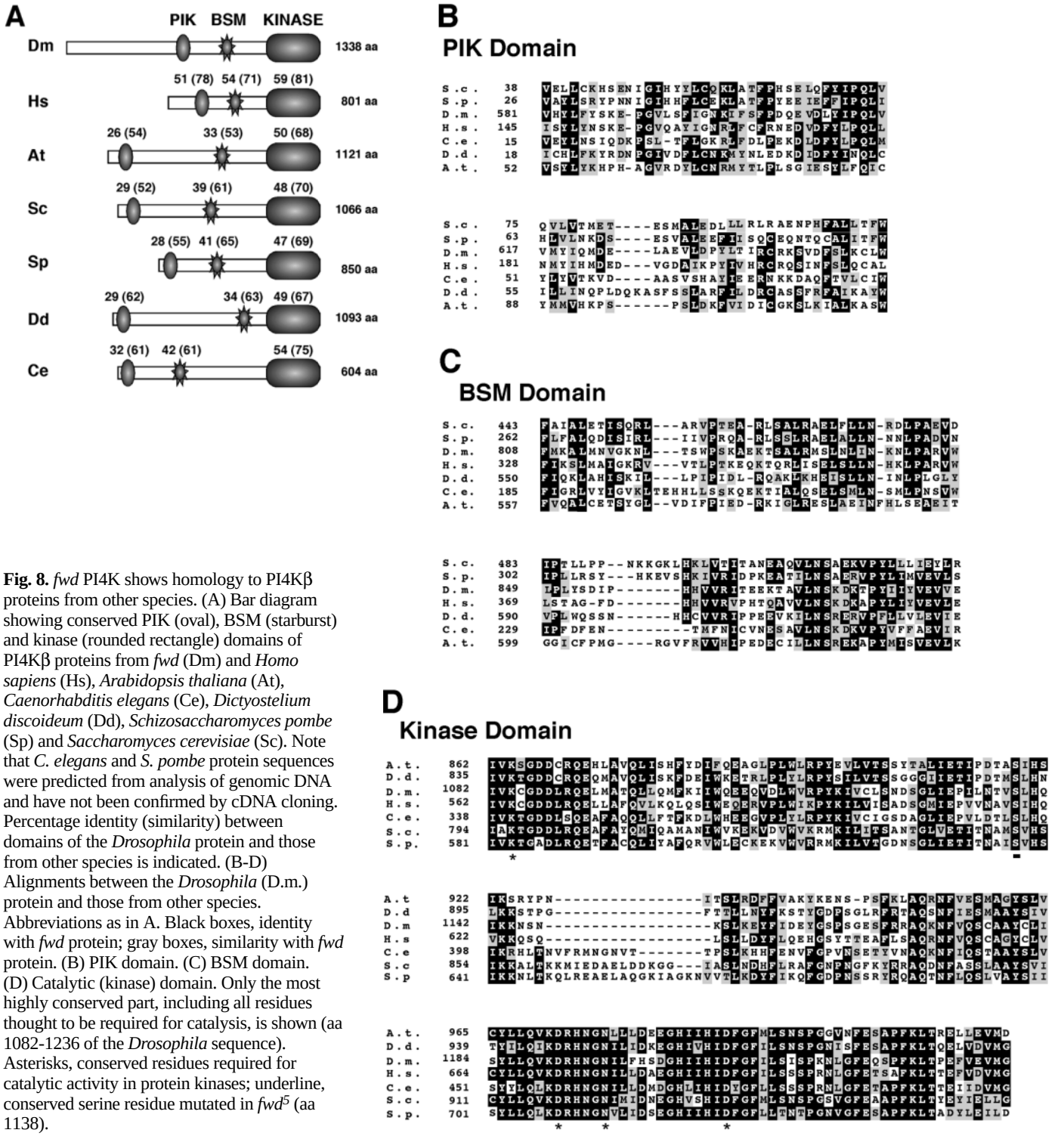

Fig. 8. *fwd* PI4K shows homology to PI4Kβ proteins from other species. (A) Bar diagram showing conserved PIK (oval), BSM (starburst) and kinase (rounded rectangle) domains of PI4Kβ proteins from *fwd* (Dm) and *Homo sapiens* (Hs), *Arabidopsis thaliana* (At), *Caenorhabditis elegans* (Ce), *Dictyostelium discoideum* (Dd), *Schizosaccharomyces pombe* (Sp) and *Saccharomyces cerevisiae* (Sc). Note that *C. elegans* and *S. pombe* protein sequences were predicted from analysis of genomic DNA and have not been confirmed by cDNA cloning. Percentage identity (similarity) between domains of the *Drosophila* protein and those from other species is indicated. (B-D) Alignments between the *Drosophila* (D.m.) protein and those from other species. Abbreviations as in A. Black boxes, identity with *fwd* protein; gray boxes, similarity with *fwd* protein. (B) PIK domain. (C) BSM domain. (D) Catalytic (kinase) domain. Only the most highly conserved part, including all residues thought to be required for catalysis, is shown (aa 1082-1236 of the *Drosophila* sequence). Asterisks, conserved residues required for catalytic activity in protein kinases; underline, conserved serine residue mutated in *fwd*^{5} (aa 1138).

fwd PI4K may link membrane trafficking with constriction of the contractile ring

Precedents from other organisms suggest that loss of *fwd* function could lead to defects in membrane trafficking and phosphoinositide accumulation required for normal resolution of cytokinesis. Vesicle fusion during cleavage furrow formation in *Xenopus* oocytes and *Caenorhabditis elegans* embryos (Drechsel et al., 1997; Danilchik et al., 1998; Jantsch-Plunger and Glotzer, 1999) provides protein and phospholipid to the enlarging plasma membrane surface as cytokinesis progresses. Yeast and human homologs of *fwd* PI4Kβ proteins are implicated in secretion and membrane vesicle trafficking, consistent with accumulating evidence that PIP2 participates in these processes (reviewed by Balla, 1998; Hsuan et al., 1998). Yeast two-hybrid experiments and double mutant analysis detected both physical and functional interactions

between PIK1 and FRQ1 (Hendricks et al., 1999), the yeast homolog of *Drosophila* frequenin, which modulates synaptic vesicle fusion events at nerve termini (Pongs et al., 1993). The human homolog of *fwd*, PI4Kβ, requires ARF, a small GTPase involved in budding of vesicles from the Golgi, for its Golgi localization and activity (Rothman and Wieland, 1996; Schekman and Orci, 1996; Nakagawa et al., 1996; Wong et al., 1997; Godi et al., 1999). Because dominant negative PI4Kβ causes Golgi disorganization in human tissue culture cells (Godi et al., 1999), it has been proposed that local distribution of phosphoinositides activates ARF and mediates membrane skeleton reorganization to permit formation and secretion of Golgi-derived vesicles (Terui et al., 1994; Godi et al., 1999; Lorra and Huttner, 1999). These vesicles, in turn, could be targeted to the cleavage furrow during cytokinesis.

fwd may stabilize interactions between contractile ring proteins and the plasma membrane. PIP2 and PIP3 bind proteins with PH domains (Harlan et al., 1994; Ma et al., 1997; Rameh et al., 1997; Varnai and Balla, 1998; Varnai et al., 1999). *fwd*-dependent local accumulation of PIP2 or PIP3 could anchor PH domain-containing contractile ring proteins, such as anillin (Field and Alberts, 1995), to the plasma membrane. Likewise, septins, which contain a conserved polybasic domain that binds PIP2 and PIP3 (Zhang et al., 1999), may require *fwd* to maintain their cleavage furrow association. Disruption of the membrane binding of these actin-associated proteins could lead to disorganization of F-actin in *fwd* mutant flies. Because of its potential to regulate both vesicle trafficking and membrane-cytoskeletal interactions, the *fwd* PI4K may coordinate contractile ring function with membrane addition during cytokinesis.

Activity of *fwd* is required for appearance of phosphotyrosine epitopes in the constricting cleavage furrow. Intriguingly, distribution of PH domain-containing *src*-related tyrosine kinases such as Btk appears to be controlled by PIP2 or PIP3 localization (Harlan et al., 1994; Varnai and Balla, 1998; Varnai et al., 1999). The failure of P-tyr epitopes to accumulate on contractile rings in *fwd* mutant spermatocytes may reflect the absence of phosphoinositides that serve as essential localization signals for the relevant tyrosine kinase(s). Alternatively, the defect in P-tyr accumulation in *fwd* could be due to failure to bring the kinase and its substrate together. For example, the kinase could be localized to the membrane and the substrate to the contractile ring. If these two structures failed to maintain contact during constriction, no tyrosine phosphorylation would take place. *fwd*-dependent tyrosine phosphorylation of a target protein could be a key regulatory event governing ring canal stabilization in the male germline of *Drosophila*.

The authors thank Lynn Cooley and Allan Spradling for the fwd^1 allele, Nurit Wolf for her excellent technical assistance in the initial characterization of fwd^1, Jim Posakony for deficiency stocks, Bill Gelbart for the Δ2-3 line, Dan Kiehart for the anti-myosin II antibody, Justen Andrew and Brian Oliver for the BS testis cDNA library, and members of the Baker and Schubiger labs for generously allowing us to use their microscopes. J. A. B. gratefully acknowledges Barbara Wakimoto for advice and encouragement, and for providing facilities to carry out the latter stages of these experiments, Craig Waters for assistance with the P-element mutagenesis screen, Salli Tazuke for her Northern blot, Lekha Devarayalu of the Biochemistry Sequencing Facility at the University of Washington for assistance with genomic sequencing and members of the Fuller and Wakimoto labs for excellent discussions. Many kind thanks to John Ashkenas, Lynn Cooley, Rebecca Farkas, Karen Hales, Rachel Meyers, Barbara Wakimoto and Philippa Webster for helpful comments on the manuscript. J. A. B. was supported by an NIH National Research Service Award #5-F32-HD07728, a Katharine McCormick Fellowship from Stanford University and a Special Fellowship of the Leukemia and Lymphoma Society. G. R. H. was supported by C. J. Martin Fellowship #937316 from the National Health and Medical Research Council of Australia and a Walter V. and Idun Y. Berry Fellowship from Stanford University. M. S.-S. was an American Heart Association-California Affiliate summer student. This work was funded by NIH grants RO1-HD18127 and RO1-HD29194 to M. T. F.

REFERENCES

Adachi, H., Takahashi, Y., Hasebe, T., Shirouzu, M., Yokoyama, S. and Sutoh, K. (1997). Dictyostelium IQGAP-related protein specifically involved in the completion of cytokinesis. *J. Cell Biol*. **137**, 891-898.

Ashburner, M. (1990). *Drosophila: A Laboratory Handbook.* Cold Spring Harbor, NY: Cold Spring Harbor Press.

Balla, T. (1998). Phosphatidylinositol 4-kinases. *Biochim. Biophys. Acta* **1436**, 69-85.

Cenci, G., Bonaccorsi, S., Pisano, C., Verni, F. and Gatti, M. (1994). Chromatin and microtubule organization during premeiotic, meiotic and early postmeiotic stages of Drosophila melanogaster spermatogenesis. *J. Cell Sci*. **107**, 3521-3534.

Church, K. and Lin, H. P. (1985). Kinetochore microtubules and chromosome movement during prometaphase in Drosophila melanogaster spermatocytes studied in life and with the electron microscope. *Chromosoma* **92**, 273-282.

Cooley, L. (1995). Oogenesis: variations on a theme. *Dev. Genet.* **16**, 1-5.

Cooley, L., Kelley, R. and Spradling, A. (1988). Insertional mutagenesis of the Drosophila genome with single P elements. *Science* **239**, 1121-1128.

Danilchik, M. V., Funk, W. C., Brown, E. E. and Larkin, K. (1998). Requirement for microtubules in new membrane formation during cytokinesis of Xenopus embryos. *Dev. Biol*. **194**, 47-60.

Deak, P., Omar, M. M., Saunders, R. D., Pal, M., Komonyi, O., Szidonya, J., Maroy, P., Zhang, Y., Ashburner, M., Benos, P., et al. (1997). P-element insertion alleles of essential genes on the third chromosome of Drosophila melanogaster: correlation of physical and cytogenetic maps in chromosomal region 86E-87F. *Genetics* **147**, 1697-1722.

Drechsel, D. N., Hyman, A. A., Hall, A. and Glotzer, M. (1997). A requirement for Rho and Cdc42 during cytokinesis in Xenopus embryos. *Curr. Biol*. **7**, 12-23.

Field, C., Li, R. and Oegema, K. (1999). Cytokinesis in eukaryotes: a mechanistic comparison. *Curr. Opin. Cell Biol*. **11**, 68-80.

Field, C. M. and Alberts, B. M. (1995). Anillin, a contractile ring protein that cycles from the nucleus to the cell cortex. *J. Cell Biol*. **131**, 165-178.

Fishkind, D. J. and Wang, Y. L. (1995). New horizons for cytokinesis. *Curr. Opin. Cell Biol*. **7**, 23-31.

Flanagan, C. A., Schnieders, E. A., Emerick, A. W., Kunisawa, R., Admon, A. and Thorner, J. (1993). Phosphatidylinositol 4-kinase: gene structure and requirement for yeast cell viability. *Science* **262**, 1444-1448.

Fruman, D. A., Meyers, R. E. and Cantley, L. C. (1998). Phosphoinositide kinases. *Annu Rev. Biochem.* **67**, 481-507.

Fuller, M. T. (1993). Spermatogenesis. In *The Development of Drosophila* (ed. M. Bate and A. Martinez-Arias), pp. 71-147. Cold Spring Harbor, NY: Cold Spring Harbor Press.

Garcia-Bustos, J. F., Marini, F., Stevenson, I., Frei, C. and Hall, M. N. (1994). PIK1, an essential phosphatidylinositol 4-kinase associated with the yeast nucleus. *Embo J*. **13**, 2352-2361.

Gehrmann, T. and Heilmeyer, Jr., L. M. (1998). Phosphatidylinositol 4-kinases. *Eur. J. Biochem.* **253**, 357-370.

Giansanti, M. G., Bonaccorsi, S., Williams, B., Williams, E. V., Santolamazza, C., Goldberg, M. L. and Gatti, M. (1998). Cooperative interactions between the central spindle and the contractile ring during Drosophila cytokinesis. *Genes Dev.* **12**, 396-410.

Godi, A., Pertile, P., Meyers, R., Marra, P., Di Tullio, G., Iurisci, C., Luini, A., Corda, D. and De Matteis, M. A. (1999). ARF mediates recruitment of PtdIns-4-OH kinase-β and stimulates synthesis of PtdIns(4,5)P_2 on the

Golgi complex. *Nature Cell Biol*. **1**, 280-287.
Gonzalez, C., Casal, J. and Ripoll, P. (1989). Relationship between chromosome content and nuclear diameter in early spermatids of Drosophila melanogaster. *Genet. Res*. **54**, 205-212.
Gunsalus, K. C., Bonaccorsi, S., Williams, E., Verni, F., Gatti, M. and Goldberg, M. L. (1995). Mutations in twinstar, a Drosophila gene encoding a cofilin/ADF homologue, result in defects in centrosome migration and cytokinesis. *J. Cell Biol*. **131**, 1243-1259.
Harlan, J. E., Hajduk, P. J., Yoon, H. S. and Fesik, S. W. (1994). Pleckstrin homology domains bind to phosphatidylinositol-4,5-bisphosphate. *Nature* **371**, 168-170.
Hendricks, K. B., Wang, B. Q., Schnieders, E. A. and Thorner, J. (1999). Yeast homologue of neuronal frequenin is a regulator of phosphatidylinositol-4-OH kinase. *Nature Cell Biol*. **1**, 234-241.
Hime, G. R., Brill, J. A. and Fuller, M. T. (1996). Assembly of ring canals in the male germ line from structural components of the contractile ring. *J. Cell Sci*. **109**, 2779-2788.
Hsuan, J. J., Minogue, S. and dos Santos, M. (1998). Phosphoinositide 4- and 5-kinases and the cellular roles of phosphatidylinositol 4,5-bisphosphate. *Adv. Cancer Res*. **74**, 167-216.
Isaac, D. D. and Andrew, D. J. (1996). Tubulogenesis in Drosophila: a requirement for the trachealess gene product. *Genes Dev*. **10**, 103-117.
Jantsch-Plunger, V. and Glotzer, M. (1999). Depletion of syntaxins in the early Caenorhabditis elegans embryo reveals a role for membrane fusion events in cytokinesis. *Curr. Biol*. **9**, 738-745.
Lehmann, R. and Nusslein-Volhard, C. (1986). Abdominal segmentation, pole cell formation, and embryonic polarity require the localized activity of oskar, a maternal gene in Drosophila. *Cell* **47**, 141-152.
Lin, T. Y., Viswanathan, S., Wood, C., Wilson, P. G., Wolf, N. and Fuller, M. T. (1996). Coordinate developmental control of the meiotic cell cycle and spermatid differentiation in Drosophila males. *Development* **122**, 1331-1341.
Lindsley, D. and Tokuyasu, K. T. (1980). Spermatogenesis. In *Genetics and Biology of* Drosophila (ed. M. Ashburner and T.R. Wright), pp. 225-94. New York: Academic Press.
Lindsley, D. L. and Zimm, G. G. (1992). *The Genome of Drosophila melanogaster*. San Diego: Academic Press.
Longtine, M. S., DeMarini, D. J., Valencik, M. L., Al-Awar, O. S., Fares, H., De Virgilio, C. and Pringle, J. R. (1996). The septins: roles in cytokinesis and other processes. *Curr. Opin. Cell Biol*. **8**, 106-119.
Lorra, C. and Huttner, W. B. (1999). The mesh hypothesis of Golgi dynamics. *Nature Cell Biol*. **1**, E113-115.
Ma, A. D., Brass, L. F. and Abrams, C. S. (1997). Pleckstrin associates with plasma membranes and induces the formation of membrane projections: requirements for phosphorylation and the NH2- terminal PH domain. *J. Cell Biol*. **136**, 1071-1079.
Madaule, P., Eda, M., Watanabe, N., Fujisawa, K., Matsuoka, T., Bito, H., Ishizaki, T. and Narumiya, S. (1998). Role of citron kinase as a target of the small GTPase Rho in cytokinesis. *Nature* **394**, 491-494.
Nakagawa, T., Goto, K. and Kondo, H. (1996). Cloning and characterization of a 92 kDa soluble phosphatidylinositol 4- kinase. *Biochem. J*. **320**, 643-649.
O'Connell, P. O. and Rosbash, M. (1984). Sequence, structure, and codon preference of the Drosophila ribosomal protein 49 gene. *Nucleic Acids Res*. **12**, 5495-5513.
Pongs, O., Lindemeier, J., Zhu, X. R., Theil, T., Engelkamp, D., Krah-Jentgens, I., Lambrecht, H. G., Koch, K. W., Schwemer, J., Rivosecchi, R. et al. (1993). Frequenin–a novel calcium-binding protein that modulates synaptic efficacy in the Drosophila nervous system. *Neuron* **11**, 15-28.
Powers, J., Bossinger, O., Rose, D., Strome, S. and Saxton, W. (1998). A nematode kinesin required for cleavage furrow advancement. *Curr. Biol*. **8**, 1133-1136.
Preston, C.R., Sved, J. A. and Engels, W. R. (1996). Flanking duplications and deletions associated with P-induced male recombination in Drosophila. *Genetics* **144,** 1623-1638.
Raich, W. B., Moran, A. N., Rothman, J. H. and Hardin, J. (1998). Cytokinesis and midzone microtubule organization in Caenorhabditis elegans require the kinesin-like protein ZEN-4. *Mol. Biol. Cell* **9**, 2037-2049.
Rameh, L. E., Arvidsson, A., Carraway, 3rd, K. L., Couvillon, A. D., Rathbun, G., Crompton, A., VanRenterghem, B., Czech, M. P., Ravichandran, K. S., Burakoff, S. J., Wang, D. S., Chen, C. S. and Cantley, L. C. (1997). A comparative analysis of the phosphoinositide binding specificity of pleckstrin homology domains. *J. Biol Chem*. **272**, 22059-22066.
Regan, C. L. and Fuller, M. T. (1990). Interacting genes that affect microtubule function in Drosophila melanogaster: two classes of mutation revert the failure to complement between haync2 and mutations in tubulin genes. *Genetics* **125**, 77-90.
Rothman, J. E. and Wieland, F. T. (1996). Protein sorting by transport vesicles. *Science* **272**, 227-234.
Sambrook, J., Fritsch, E. F. and Maniatis, T. (1989). *Molecular Cloning: A Laboratory Manual*. Cold Spring Harbor, NY: Cold Spring Harbor Press.
Satterwhite, L. L. and Pollard, T. D. (1992). Cytokinesis. *Curr. Opin. Cell Biol*. **4**, 43-52.
Schekman, R. and Orci, L. (1996). Coat proteins and vesicle budding. *Science* **271**, 1526-1533.
Swan, K. A., Severson, A. F., Carter, J. C., Martin, P. R., Schnabel, H., Schnabel, R. and Bowerman, B. (1998). cyk-1: a C. elegans FH gene required for a late step in embryonic cytokinesis. *J. Cell Sci*. **111**, 2017-2027.
Tamkun J. W., Deuring, R., Scott, M. P., Kissinger, M., Pattatucci, A. M., Kaufman, T. C. and Kennison, J. A. (1992). brahma: a regulator of Drosophila homeotic genes structurally related to the yeast transcriptional activator SNF2/SWI2. *Cell* **68**, 561-72.
Terui, T., Kahn, R. A. and Randazzo, P. A. (1994). Effects of acid phospholipids on nucleotide exchange properties of ADP- ribosylation factor 1. Evidence for specific interaction with phosphatidylinositol 4,5-bisphosphate. *J. Biol Chem*. **269**, 28130-28135.
Uemura, T., Shepherd, S., Ackerman, L., Jan, L. Y. and Jan, Y. N. (1989). numb, a gene required in determination of cell fate during sensory organ formation in Drosophila embryos. *Cell* **58**, 349-360.
Varnai, P. and Balla, T. (1998). Visualization of phosphoinositides that bind pleckstrin homology domains: calcium- and agonist-induced dynamic changes and relationship to myo-[3H]inositol-labeled phosphoinositide pools. *J. Cell Biol*. **143**, 501-510.
Varnai, P., Rother, K. I. and Balla, T. (1999). Phosphatidylinositol 3-kinase-dependent membrane association of the Bruton's tyrosine kinase pleckstrin homology domain visualized in single living cells. *J. Biol. Chem*. **274**, 10983-10989.
White-Cooper, H., Schafer, M. A., Alphey, L. S. and Fuller, M. T. (1998). Transcriptional and post-transcriptional control mechanisms coordinate the onset of spermatid differentiation with meiosis I in Drosophila. *Development* **125**, 125-134.
Williams, B. C., Riedy, M. F., Williams, E. V., Gatti, M. and Goldberg, M. L. (1995). The Drosophila kinesin-like protein KLP3A is a midbody component required for central spindle assembly and initiation of cytokinesis. *J. Cell Biol*. **129**, 709-723.
Wong, K., Meyers, R. and Cantley, L. C. (1997). Subcellular locations of phosphatidylinositol 4-kinase isoforms. *J. Biol. Chem*. **272**, 13236-13241.
Xue, H. W., Pical, C., Brearley, C., Elge, S. and Muller-Rober, B. (1999). A plant 126-kDa phosphatidylinositol 4-kinase with a novel repeat structure. Cloning and functional expression in baculovirus-infected insect cells. *J. Biol Chem*. 274, 5738-5745.
Zhang, J., Kong, C., Xie, H., McPherson, P. S., Grinstein, S. and Trimble, W. S. (1999). Phosphatidylinositol polyphosphate binding to the mammalian septin H5 is modulated by GTP. *Curr. Biol.* **9**, 1458-67
Zhang, P. and Spradling, A. C. (1993). Efficient and dispersed local P element transposition from Drosophila females. *Genetics* **133**, 361-373.